



© 2024 Geological Society of America. For permission to copy, contact editing@geosociety.org.

Manuscript received 25 February 2024 Revised manuscript received 22 April 2024 Manuscript accepted 10 May 2024

Published online 23 May 2024

# Early Mississippian global $\delta^{13}$ C excursion is not a diagenetic artifact

Matthew G. Braun<sup>1</sup>, Noah T. Anderson<sup>2</sup>, Kristin D. Bergmann<sup>2</sup>, Elizabeth M. Griffith<sup>1</sup>, and Matthew R. Saltzman<sup>1,\*</sup>

<sup>1</sup>School of Earth Sciences, Ohio State University, 125 South Oval Mall, Columbus, Ohio 43210, USA

<sup>2</sup>Department of Earth, Atmospheric, and Planetary Sciences, Massachusetts Institute of Technology, 77 Massachusetts Avenue, Cambridge, Massachusetts 02139, USA

## **ABSTRACT**

Shallow-water platform carbonate  $\delta^{13}C$  may provide a record of changes in ocean chemistry through time, but early marine diagenesis and local processes can decouple these records from the global carbon cycle. Recent studies of calcium isotopes ( $\delta^{44/40}Ca$ ) in shallow-water carbonates indicate that  $\delta^{44/40}Ca$  can be altered during early marine diagenesis, implying that  $\delta^{13}C$  may also potentially be altered. Here, we tested the hypothesis that the platform carbonate  $\delta^{13}C$  record of the Kinderhookian–Osagean boundary excursion (KOBE), ~353 m.y. ago, reflects a period of global diagenesis using paired isotopic ( $\delta^{44/40}Ca$  and clumped isotopes) and trace-element geochemistry from three sections in the United States. There is little evidence for covariation between  $\delta^{44/40}Ca$  and  $\delta^{13}C$  during the KOBE. Clumped isotopes from our shallowest section support primarily sediment-buffered diagenesis at relatively low temperatures. We conclude that the  $\delta^{13}C$  record of the KOBE as recorded in shallow-water carbonate is consistent with a shift in the dissolved inorganic carbon reservoir and that, more generally, ancient shallow-water carbonates can retain records of primary seawater chemistry.

## INTRODUCTION

Shallow-water carbonate rocks are a storehouse of geochemical information that can be used to decipher cause-and-effect relationships within the ocean-atmosphere-biosphere system through Earth history. Carbon isotopes ( $\delta^{13}$ C) in carbonate rocks are used as both a proxy for the ancient carbon (C) cycle and for chronostratigraphic correlations, with the assumption that a primary marine signal is recorded (Kump and Arthur, 1999). However, recognition that Neogene shallow-water carbonates do not track global ocean δ<sup>13</sup>C (Swart, 2008) calls into question whether pre-Mesozoic carbon isotope excursions (CIEs) were related to the global C cycle. Recent work on early marine diagenesis using calcium isotopes ( $\delta^{44/40}$ Ca; Higgins et al., 2018) has reinvigorated discussion about the role of diagenesis in producing spatial or temporal changes in  $\delta^{13}$ C in ancient shallow-water carbonates.

Paired  $\delta^{44/40}$ Ca and Sr/Ca investigation is a powerful tool to assess the extent and style of

Matthew R. Saltzman https://orcid.org/0000-0001-8052-1399

\*saltzman.11@osu.edu

early marine diagenesis in carbonate rocks (Fantle and Higgins, 2014; Lau et al., 2017; Higgins et al., 2018), and it is complemented by clumped isotope thermometry (TD47; Staudigel et al., 2021). In modern carbonates,  $\delta^{44/40}$ Ca and Sr/ Ca are primarily determined by carbonate mineralogy (aragonite vs. calcite) and precipitation rate (Gussone et al., 2005; Tang et al., 2008), whereas clumped isotopes respond to temperature and are unaffected by changes in carbonate polymorph and precipitation rate when minerals form in isotopic equilibrium (Eiler, 2011; Fiebig et al., 2021). Aragonite is depleted in <sup>44</sup>Ca (offset  $\sim$  -0.6% from calcite), and fast-forming minerals have lower  $\delta^{44/40}$ Ca compared to slowforming diagenetic minerals (Gussone et al., 2005; Fantle and DePaolo, 2007). Aragonite is enriched in Sr/Ca compared to calcite, and Sr is depleted during neomorphism and dolomitization (Ahm et al., 2018). While all carbonate sediments are subject to early marine diagenesis, the water-rock ratio is a major control on the extent to which the geochemical signature is altered (Fantle and DePaolo, 2007; Higgins et al., 2018) and can be characterized between sediment-buffered (low water-rock ratio) and

fluid-buffered (high water-rock ratio) end members (Ahm et al., 2018). Primary isotopic compositions will be retained under sedimentbuffered conditions, and  $\Delta_{47}$  will plot along a mineral contour as  $\delta^{18}O_{mineral}$  values remain unchanged (Bergmann et al., 2018). Under fluidbuffered conditions, sediments will be altered toward seawater values ( $\uparrow \delta^{44/40}$ Ca,  $\downarrow \delta^{13}$ C), and  $T\Delta_{47}$  will plot transverse to mineral contours as δ<sup>18</sup>O<sub>mineral</sub> values are altered. Thus, if covariation is observed between  $\delta^{\mbox{\tiny 44/40}}\mbox{Ca}$  and  $\delta^{\mbox{\tiny 13}}\mbox{C},$  this most likely reflects changes in the style of diagenesis or a shift in mineralogy rather than seawater chemistry because of the much longer oceanic residence time of Ca compared to C (Ahm et al., 2018).

Early Mississippian shallow-marine carbonates worldwide record a pronounced positive shift in  $\delta^{13}$ C known as the Kinderhookian–Osagean boundary excursion (KOBE) or Tournaisian carbon isotope excursion (TICE), one of the largest positive  $\delta^{13}$ C excursions of the Phanerozoic of +7‰ (Saltzman, 2003; Chen et al., 2021). The KOBE has been documented in the United States (Saltzman, 2003; Maharjan et al., 2018; Oehlert et al., 2019; Myrow et al., 2023; Braun et al., 2023; Quinton et al., 2023), Europe (Saltzman et al., 2004), and China (Yao et al., 2015; Chen et al., 2021), coincident with a  $\delta^{18}$ O increase in brachiopod calcite and conodont apatite consistent with global cooling near the onset of the Late Paleozoic ice age (Fig. 1; Mii et al., 1999; Yao et al., 2015; Chen et al., 2021).

Our study aimed to test the hypothesis that the KOBE reflects a globally synchronous shift between fluid-buffered and sediment-buffered early marine diagenesis. We present paired  $\delta^{13} C, \delta^{44/40} Ca$ , and Sr/Ca data from three localities to better understand the role of diagenesis. At our shallowest buried section in Iowa,  $\Delta_{47}$  was measured and supplemented by petrographic analysis for additional constraints on diagenesis.

CITATION: Braun, M.G., et al., 2024, Early Mississippian global  $\delta^{13}$ C excursion is not a diagenetic artifact: Geology, v. XX, p. .1130/G52109.1

, https://doi.org/10

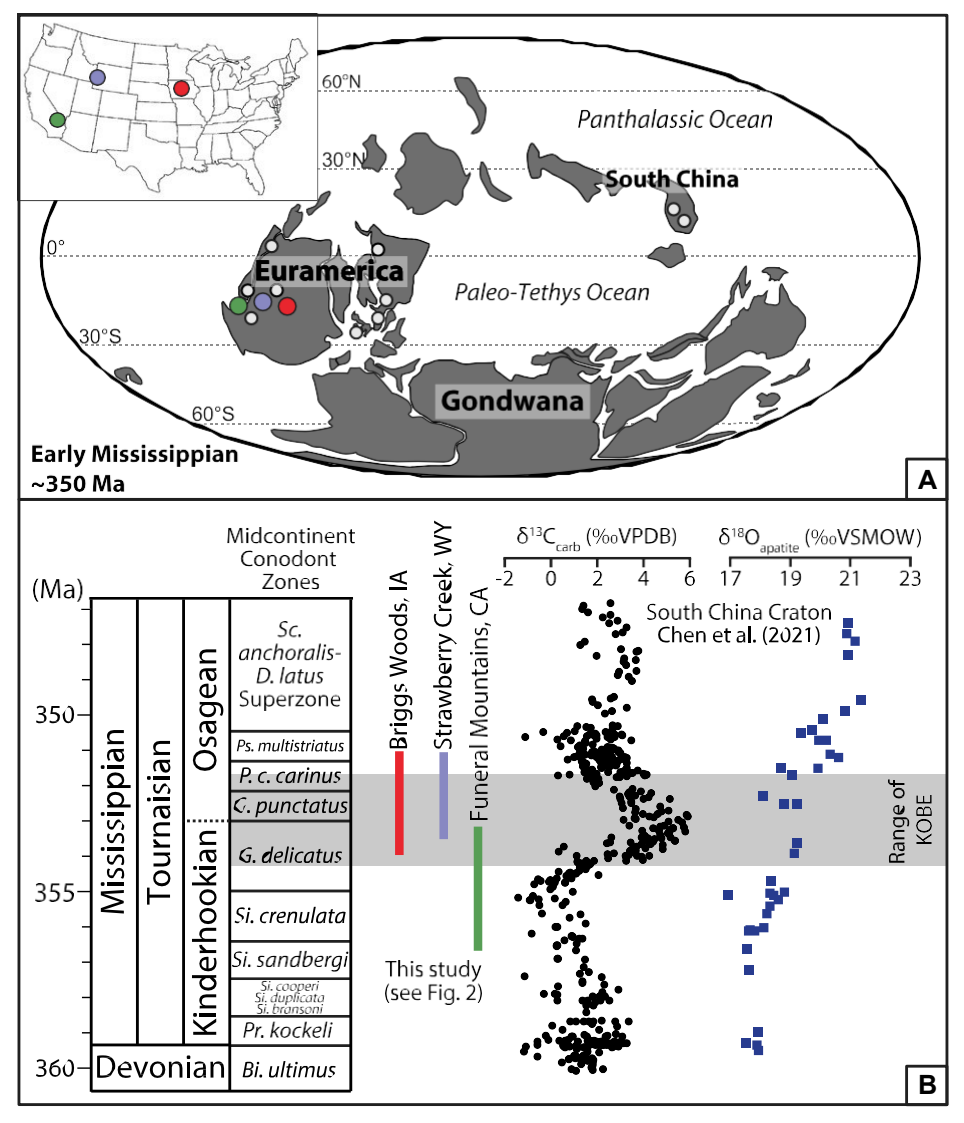


Figure 1. (A) Paleogeographic map during the Early Mississippian showing study sites at Briggs Woods (red), Strawberry Creek (blue), and Funeral Mountains (green). Select Kinderhookian–Osagean boundary excursion (KOBE) sections in North America, Europe, and China are indicated by gray circles demonstrating global nature. (B) C and O isotopic trends from South China craton (Chen et al., 2021) with approximate range of KOBE and our study sections (δ¹³C not plotted here; see Fig. 2). Midcontinent conodont zones are from Braun et al. (2023). IA—lowa; WY—Wyoming; CA—California; VPDB—Vienna Peedee belemnite; VSMOW—Vienna standard mean ocean water. Conodont genera abbreviations: Bi.—Bispathodus; D.—Doliognathus; G.—Gnathodus; P.—Polygnathus; Pr.—Protognathodus; Ps.—Pseudopolygnathus; Sc.—Scaliognathus; Si.—Siphonodella.

## **METHODS**

Early Mississippian sections (Briggs Woods, Iowa, and Strawberry Creek, Wyoming; Fig. 1), in which the KOBE had been previously identified (Saltzman, 2003; Braun et al., 2023), and one new section (Funeral Mountains, California) were chosen to represent a range of depositional environments (Fig. 2). Although the sections are not complete, together they capture the full range of KOBE  $\delta^{13}$ C variation and allow us to test the hypothesis of covariation with  $\delta^{44/40}$ Ca. Importantly, the choice of sections provided a range of lithologies representing different grain sizes, water depths, and sedimentation rates during the KOBE. We also sought to minimize dolomitized

intervals, which are common, and which limited us to certain localities and stratigraphic intervals within the sections (e.g., most of Maynes Creek at Briggs Woods below where we began sampling is dolomitized). Briggs Woods is an inner-shelf carbonate unit dominated by skeletal-oolitic and peloidal packstones and grainstones (Braun et al., 2023). Strawberry Creek is dominated by mudstones and skeletal packstones deposited below fair-weather wave base in a middle-ramp environment (Saltzman, 2003). Funeral Mountains represents an outer-shelf environment with lime mudstones and skeletal wackestones interbedded with tempestite grainstones; the KOBE is recorded here in flanking beds of Waulsortian-type mud mounds.

Bulk carbonate powders were digested and analyzed for elemental concentrations (Ca, Sr, Mg) and  $\delta^{44/40}$ Ca. A double-spike technique was used on a thermal ionization mass spectrometer to determine  $\delta^{44/40}$ Ca (‰), and results are reported relative to modern seawater (SW). External reproducibility of SRM-915a and SRM-915b yielded values of  $-1.88\% \pm 0.06\%$  $(n = 17, 2\sigma)$  and  $-1.14\% \pm 0.08\%$  (n = 12, $2\sigma$ ), respectively. Splits of seven sample powders were randomly selected and analyzed to confirm homogeneity, with average reproducibility of  $\pm 0.04\%$  (2 $\sigma$ ); replicate analyses of samples were on average  $\pm 0.09\%$  (n = 17). Clumped isotopic measurements followed the methods of Anderson et al. (2021) using a Nu Perspective isotope ratio mass spectrometer (IRMS) and carbonate-based standardization with a 1:1 unknown:anchor ratio. Pooled  $\Delta_{47}$ external repeatability (1 SD) of standards and samples, including error associated with construction of the reference frame, was 0.022‰.

#### RESULTS

Our study sections record  $\delta^{44/40}$ Ca and Sr/ Ca ranges of -1.17% to -0.74% and 0.10-0.37 mmol/mol at Briggs Woods, -1.18‰ to -0.89‰ and 0.10-0.81 mmol/mol at Strawberry Creek, and -1.18% to -0.99% and 0.18– 0.59 mmol/mol at Funeral Mountains, respectively (Fig. 2; see Supplemental Material<sup>1</sup>). When  $\delta^{13}$ C increased to peak values, no significant covariation was observed with  $\delta^{44/40}$ Ca and Sr/Ca (Fig. 3). T $\Delta_{47}$ values at Briggs Woods range from 11 to 54 °C in limestones (avg. 36 °C; Fig. 3). While dolomitized intervals (high Mg/Ca) record elevated TΔ<sub>47</sub> values,  $\delta^{44/40}$ Ca values measured from dolostone samples in Briggs Woods (n = 1) and Strawberry Creek (n = 2) are comparable to limestone samples from the same locations.

#### DISCUSSION

Globally correlative  $\delta^{13}C$  excursions represent temporal changes in individual stratigraphic sections driven by a global process, and they also commonly show spatial variability between sections (i.e., magnitude and initial/final  $\delta^{13}C$ ) driven by local processes. Here, we discuss whether global diagenesis could have produced the KOBE  $\delta^{13}C$  excursion in stratigraphic sequences worldwide (our main goal), and we also address spatial variability.

## Stratigraphic Trends

The  $\delta^{13}$ C value changes significantly through time in our stratigraphic sections with little to

<sup>&</sup>lt;sup>1</sup>Supplemental Material. Table S1, geochemical data, and File S1, background on stratigraphic sections and geochemical methods. Please visit https://doi.org/10.1130/GEOL.S.25829482 to access the supplemental material; contact editing@geosociety.org with any questions.

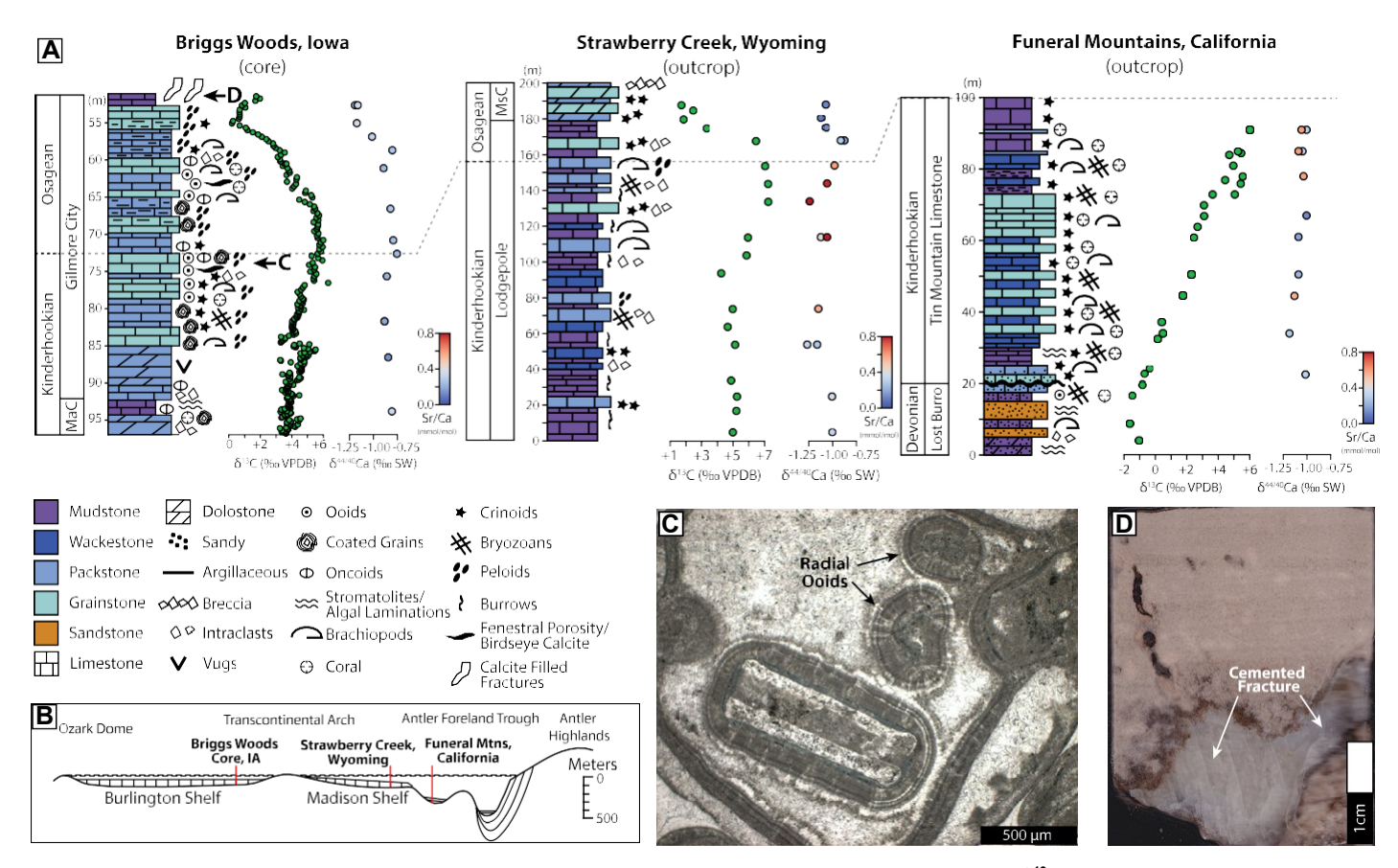


Figure 2. (A) Stratigraphic plots of geochemical data arranged by increasing water depth. Lithology and  $\delta^{13}$ C for Briggs Woods are from Braun et al. (2023); Strawberry Creek values are from Saltzman (2003); Funeral Mountains data are published here for first time. Sr/Ca scale bar applies to fill color on  $\delta^{44/40}$ Ca data points. Note that for Briggs Woods, study interval of Braun et al. (2023) begins below base of our section (see Table S1 [text footnote 1]) and includes entire Maynes Creek (MaC)–Gilmore City Formation. VPDB—Vienna Peedee belemnite; SW—seawater. (B) Schematic cross section and location of sections. (C) Thin section photomicrograph (50× magnification, 2.6 mm field of view) highlighting radial structure of ooids from Gilmore City Formation, Briggs Woods section at ~73 m. (D) Core scan of calcite-filled subvertical fracture (arrow) at ~52 m in Briggs Woods section. MsC—Mission Canyon Formation.

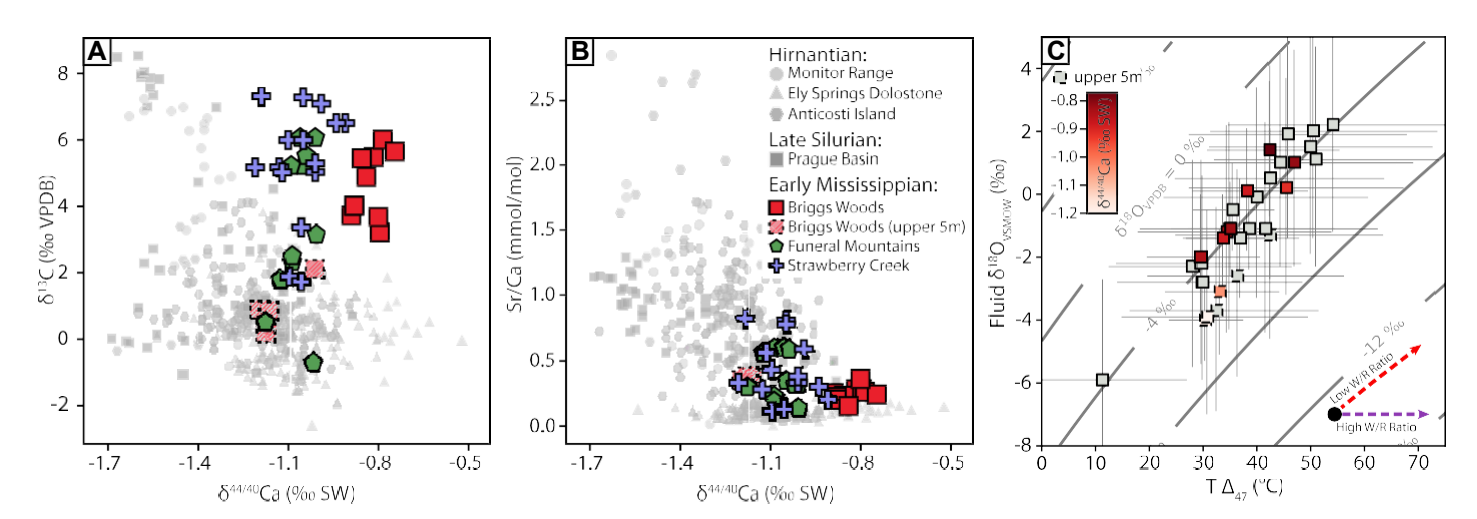


Figure 3. Cross-plots of Early Mississippian compared to Late Ordovician Hirnantian and Silurian Lau carbon isotope excursions (CIEs). Data sources: Great Basin and Anticosti (Jones et al., 2020), Monitor Range (Holmden et al., 2012a), Silurian (Farkaš et al., 2016). (A)  $\delta^{13}$ C vs.  $\delta^{44/40}$ Ca (Pearson coefficient of correlation [r] for Briggs Woods = 0.35, p value = 0.36 without upper 5 m; Funeral Mountains r = 0.44, p = 0.21; Strawberry Creek r = 0.02, p = 0.95). (B)  $\delta^{44/40}$ Ca vs. Sr/Ca. (C) Clumped isotopes from Briggs Woods showing  $\delta^{18}$ O<sub>mineral</sub> trends in T $\Delta_{47}$  and  $\delta^{18}$ Ofluid space. Arrows show predicted diagenetic trends based on water/rock (W/R) ratios (after Bergmann et al., 2018). Gray points represent T $\Delta_{47}$  without paired  $\delta^{44/40}$ Ca. Error bars on T $\Delta_{47}$  measurements are 95% confidence interval including pooled error from sample and standard measurements. VPDB—Vienna Peedee belemnite; VSMOW—Vienna standard mean ocean water; SW—seawater.

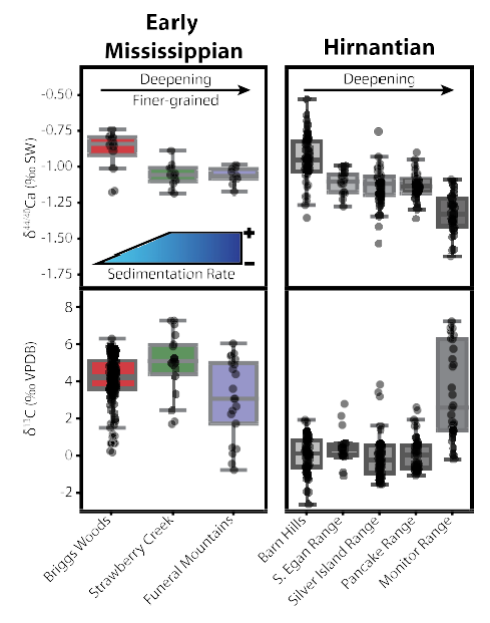


Figure 4. Box plots of Early Mississippian and Hirnantian  $\delta^{44/40}$ Ca and  $\delta^{13}$ C data (Holmden et al., 2012a; Jones et al., 2020) ordered shallowest to deepest. Note that Funeral Mountains only contains rising limb of Kinderhookian–Osagean boundary excursion (KOBE), so it is unknown if peak  $\delta^{13}$ C values above +6‰, as seen at Strawberry Creek, may potentially be reached. VPDB—Vienna Peedee belemnite; SW—seawater.

no change in  $\delta^{44/40}$ Ca (Figs. 2 and 3)—this is inconsistent with early marine diagenesis, which should result in covariation. The  $\delta^{\text{44/40}}\text{Ca}$  and Sr/ Ca values, however, may have been impacted by diagenetic alteration, but the degree depends on assumptions of original mineralogy. Because we sampled bulk carbonate, we cannot deconvolve component  $\delta^{44/40}$ Ca or original mineralogy, but previous global compilations, elemental data, and petrographic preservation, including wellpreserved radial lamellae within ooids in Briggs Woods, are consistent with calcite being a major component of our rocks (Fig. 2C; cf. Wilkinson et al., 1985). While the diagenetic model of Ahm et al. (2018) can account for the small changes in  $\delta^{44/40}$ Ca (and Sr/Ca) in our sections, the changes in  $\delta^{13}$ C are too large to fit within the model space without making assumptions about platform water mass or diagenetic fluid  $\delta^{13}$ C. In order to fit a significant portion of our data within the phase space using the Ahm et al. (2018) diagenetic model, we must begin with an assumption that our heaviest  $\delta^{13}$ C of +7% represents a minimum value for primary carbonate; however, this is problematic because such elevated  $\delta^{13}$ C predicts facies that should reflect restricted water masses (e.g., influenced by the diurnal cycle; Geyman and Maloof, 2021), but this is not what we observe. Instead, open-marine facies in our Strawberry Creek and Funeral Mountains sections record our most positive  $\delta^{13}$ C values (Fig. 2).

In terms of potential for fluid-versus sedimentbuffered diagenesis in our sections, Strawberry Creek and Funeral Mountains represent outershelf positions (Fig. 2B), which should be most affected by marine fluid-buffered diagenesis (cf. Hoffman and Lamothe, 2019), but instead they record very high, sediment-buffered δ<sup>13</sup>C values similar to Briggs Woods farther along the flow path. Meteoric groundwater influence may also have affected Briggs Woods strata (cf. Holmden et al., 2012b; Farkaš et al., 2016). Yet, 70% of clumped isotope results of limestones from Briggs Woods record temperatures below 40 °C, consistent with early (shallow) lithification, and measurements broadly follow a trajectory along a single  $\delta^{18} O_{mineral}$  contour in  $T\Delta_{47}$  and  $\delta^{18} O_{fluid}$ space for all samples except the top 5 m, discussed below (Fig. 3), consistent with early marine diagenesis under low water-rock ratio conditions (Bergmann et al., 2018; Goldberg et al., 2021). When taken as a whole, our paired  $\delta^{44/40}$ Ca and  $\Delta_{47}$  record of the KOBE is reflective of predominantly sediment-buffered diagenesis and suggests that the primary  $\delta^{13}$ C trend was not a product of early marine diagenesis.

At Briggs Woods, evidence for meteoric diagenesis is present in the top 5 m, where calcite-filled vertical fractures (Fig. 2D) are pervasive,  $\delta^{18}$ Ofluid values are depleted ( $\sim$  -4‰), and clumped isotopes plot as a separate, more fluid-buffered population (Fig. 3). Positive covariation of  $\delta^{13}$ C and  $\delta^{44/40}$ Ca in the upper 5 m at Briggs Woods (Fig. 2) is consistent with meteoric alteration (Holmden et al., 2012b). Other explanations include marine diagenesis (Ahm et al., 2021), changes in facies, or kinetic effects (Farkaš et al., 2016; Wang et al., 2023).

As no clear negative covariation was identified between  $\delta^{13}$ C and  $\delta^{44/40}$ Ca in each of our sections, which contrasts with the Late Ordovician CIE in the Monitor Range of Nevada and the falling limb of a late Silurian CIE in the Prague Basin, Czech Republic (Figs. 2 and 3), stratigraphic trends in  $\delta^{13}$ C during the KOBE do not appear to have been controlled by changes in fluid- to sediment-buffered diagenesis or primary mineralogy. Therefore, the shallow-water  $\delta^{13}$ C record most likely reflects a change in the dissolved inorganic carbon (DIC) reservoir, either due to global or local changes (Jones et al., 2020; Geyman and Maloof, 2021). Studies have linked the KOBE to elevated global marine productivity and organic C burial (Saltzman, 2003; Saltzman et al., 2004; Maharjan et al., 2018) liberated by land plants (Oehlert et al., 2019; Chen et al., 2021). Evidence for global cooling (Chen et al., 2021) and expanded ocean anoxia (Cheng et al., 2020) supports a shift in the global C cycle; however, local factors may also affect shallow environments (Geyman and Maloof, 2021). The long residence time of Ca in the oceans is consistent with the relatively invariant  $\delta^{44/40}$ Ca values over the KOBE.

## **Spatial Trends**

Diagenesis does not appear to explain the KOBE, but as is the case with nearly all CIEs, the KOBE is expressed variably in each section. Higher  $\delta^{44/40}$ Ca and lower Sr/Ca in Briggs Woods compared to deeper sections (Fig. 4) may be explained by seawater-buffered diagenesis, kinetic Ca isotopic effects, or differences in primary mineralogy. Increased seawater buffering could reflect lower sedimentation rates (Fig. 4; Staudigel et al., 2021); however, clumped isotopes at Briggs Woods do not show evidence for seawater buffering at depth, so this must have occurred early at a shallow burial depth, or other factors could have contributed to the higher  $\delta^{4440}$ Ca values there. Facies at Briggs Woods are relatively grain-rich and mud-poor facies, and pore space is predominantly infilled by cement (Fig. 2). If this cement formed slowly in equilibrium, then  $\delta^{\mbox{\tiny 44/40}}\mbox{Ca}$  would have become enriched without altering  $\Delta_{47}$ , as Ca fractionation is rate dependent, whereas clumped isotopes are not (Fiebig et al., 2021; Fantle and DePaolo, 2007; Staudigel et al., 2021). The spatial trend of higher  $\delta^{44/40}$ Ca at Briggs Woods is also evident in  $\delta^{13}$ C, where peak KOBE values are ~1% lower than at Strawberry Creek (Fig. 4) and other sections (e.g., +7%, Nevada; Cheng et al., 2020). A <sup>12</sup>C-enriched cement phase, early marine diagenetic influence, local C cycling in the shallow-water DIC pool, or facies can all contribute to spatial trends in  $\delta^{13}$ C (Saltzman et al., 2004; Holmden et al., 2012a; Geyman and Maloof, 2021; Hoffman and Lamothe, 2019).

## **CONCLUSIONS**

Our  $\delta^{44/40}$ Ca, Sr/Ca, and  $\Delta_{47}$  analyses of Early Mississippian sections suggest that ancient shallow-water platform carbonates can preserve a primary δ<sup>13</sup>C signal. No significant negative covariation was identified between  $\delta^{44/40}$ Ca and  $\delta^{13}$ C over the CIE, which suggests the KOBE in North America was not driven by a change in fluid- versus sediment-buffered diagenesis, mineralogy, or precipitation rate. This large positive  $\delta^{13}$ C excursion more likely reflects, at least in part, a significant shift in global or local DIC. Spatial variation in  $\delta^{44/40}$ Ca and  $\delta^{13}$ C between our study sections may be related to different sedimentation rates, where Briggs Woods (our shallowest section) experienced some influence of early seawater buffering on  $\delta^{44/40}$ Ca.

## ACKNOWLEDGMENTS

This work was supported by National Science Foundation grant EAR-2221962 to M.R. Saltzman and E.M. Griffith and EAR-2221963 to K.D. Bergmann. We thank A. Bancroft for assistance with sampling the Briggs Woods section, and Y.D. Adiatma and M. Fantle for discussion. We thank anonymous reviewers for constructive feedback that improved the manuscript.

### REFERENCES CITED

Ahm, A.-S.C., Bjerrum, C.J., Blättler, C.L., Swart, P.K., and Higgins, J.A., 2018, Quantifying early marine diagenesis in shallow-water carbonate

- sediments: Geochimica et Cosmochimica Acta, v. 236, p. 140–159, https://doi.org/10.1016/j.gca .2018.02.042.
- Ahm, A.-S.C., Bjerrum, C.J., Hoffman, P.F., Macdonald, F.A., Maloof, A.C., Rose, C.V., Strauss, J.V., and Higgins, J.A., 2021, The Ca and Mg isotope record of the Cryogenian Trezona carbon isotope excursion: Earth and Planetary Science Letters, v. 568, https://doi.org/10.1016/j.epsl.2021.117002.
- Anderson, N.T., Kelson, J.R., Kele, S., Daëron, M., Bonifacie, M., Horita, J., Mackey, C.M., John, C.M., Kluge, T., Petschnig, A.B., Jost, A.B., Huntington, K.W., Bernasconi, S.M., and Bergmann, K.D., 2021, A unified clumped isotope thermometer calibration (0.5–1,100 C) using carbonate-based standardization: Geophysical Research Letters, v. 48, https://doi.org/10.1029 /2020GL092069.
- Bergmann, K.D., Finnegan, S., Creel, R., Eiler, J.M., Hughes, N.C., Popov, L.E., and Fischer, W.W., 2018, A paired apatite and calcite clumped isotope thermometry approach to estimating Cambro-Ordovician seawater temperatures and isotopic composition: Geochimica et Cosmochimica Acta, v. 224, p. 18–41, https://doi.org/10.1016/j.gca.2017.11.015.
- Braun, M.G., Bancroft, A.M., Hogancamp, N.J., Stolfus, B.M., Heath, M.N., Clark, R.J., Tassier-Surine, S., Day, J.E., and Cramer, B.D., 2023, Resolving complex stratigraphic architecture across the Burlington Shelf and identifying the Hangenberg (D-C boundary) and Kinderhookian-Osagean boundary (Tournaisian) biogeochemical events in the type area of the Mississippian: Geological Society of America Bulletin, v. 136, p. 2157–2177, https://doi.org/10.1130/B36974.1.
- Chen, B., Chen, J., Qie, W., Huang, P., He, T., Joachimski, M.M., Regelous, M., Pogge von Strandmann, P.A.E., Liu, J., Wang, X., Montañez, I.P., and Algeo, T.J., 2021, Was climatic cooling during the earliest Carboniferous driven by expansion of seed plants?: Earth and Planetary Science Letters, v. 565, https://doi.org/10.1016/j .epsl.2021.116953.
- Cheng, K., Elrick, M., and Romaniello, S.J., 2020, Early Mississippian ocean anoxia triggered organic carbon burial and late Paleozoic cooling: Evidence from uranium isotopes recorded in marine limestone: Geology, v. 48, p. 363–367, https://doi.org/10.1130/G46950.1.
- Eiler, J.M., 2011, Paleoclimate reconstruction using carbonate clumped isotope thermometry: Quaternary Science Reviews, v. 30, p. 3575–3588, https://doi.org/10.1016/j.quascirev.2011.09.001.
- Fantle, M.S., and DePaolo, D.J., 2007, Ca isotopes in carbonate sediment and pore fluid from ODP Site 807A: The Ca<sup>2</sup>†<sub>(aq)</sub>—calcite equilibrium fractionation factor and calcite recrystallization rates in Pleistocene sediments: Geochimica et Cosmochimica Acta, v. 71, p. 2524–2546, https://doi.org/10.1016/j.gca.2007.03.006.
- Fantle, M.S., and Higgins, J., 2014, The effects of diagenesis and dolomitization on Ca and Mg isotopes in marine platform carbonates: Implications for the geochemical cycles of Ca and Mg: Geochimica et Cosmochimica Acta, v. 142, p. 458– 481, https://doi.org/10.1016/j.gca.2014.07.025.
- Farkaš, J., Frýda, J., and Holmden, C., 2016, Calcium isotope constraints on the marine carbon cycle and CaCO<sub>3</sub> deposition during the late Silurian (Ludfordian) positive δ<sup>13</sup>C excursion: Earth and Planetary Science Letters, v. 451, p. 31–40, https://doi.org/10.1016/j.epsl.2016.06.038; corrigendum available at https://doi.org/10.1016/j.epsl.2017.04.013.
- Fiebig, J., Daëron, M., Bernecker, M., Guo, W., Schneider, G., Boch, R., Bernasconi, S.M.,

- Jautzy, J., and Dietzel, M., 2021, Calibration of the dual clumped isotope thermometer for carbonates: Geochimica et Cosmochimica Acta, v. 312, p. 235–256, https://doi.org/10.1016/j.gca.2021.07.012.
- Geyman, E.C., and Maloof, A.C., 2021, Facies control on carbonate  $\delta^{13}$ C on the Great Bahama Bank: Geology, v. 49, p. 1049–1054, https://doi.org/10.1130/G48862.1.
- Goldberg, S.L., Present, T.M., Finnegan, S., and Bergmann, K.D., 2021, A high-resolution record of early Paleozoic climate: Proceedings of the National Academy of Sciences of the United States of America, v. 118, https://doi.org/10.1073/pnas.2013083118.
- Gussone, N., Böhm, F., Eisenhauer, A., Dietzel, M., Heuser, A., Teichert, B.M., Reitner, J., Worheide, G., and Dullo, W.C., 2005, Calcium isotope fractionation in calcite and aragonite: Geochimica et Cosmochimica Acta, v. 69, p. 4485–4494, https://doi.org/10.1016/j.gca.2005.06.003.
- Higgins, J.A., Blättler, C.L., Lundstrom, E.A., Santiago-Ramos, D.P., Akhtar, A.A., Ahm, A.-S.C., Bialik, O., Holmden, C., Bradbury, H., Murray, S.T., and Swart, P.K., 2018, Mineralogy, early marine diagenesis, and the chemistry of shallowwater carbonate sediments: Geochimica et Cosmochimica Acta, v. 220, p. 512–534, https://doi.org/10.1016/j.gca.2017.09.046.
- Hoffman, P.F., and Lamothe, K.G., 2019, Seawater-buffered diagenesis, destruction of carbon isotope excursions, and the composition of DIC in Neoproterozoic oceans: Proceedings of the National Academy of Sciences of the United States of America, v. 116, p. 18,874–18,879, https://doi.org/10.1073/pnas.1909570116.
- Holmden, C., Panchuk, K., and Finney, S.C., 2012a, Tightly coupled records of Ca and C isotope changes during the Hirnantian glaciation event in an epeiric sea setting: Geochimica et Cosmochimica Acta, v. 98, p. 94–106, https://doi.org/10 .1016/j.gca.2012.09.017.
- Holmden, C., Papanastassiou, D.A., Blanchon, P., and Evans, S., 2012b, δ<sup>44/40</sup>Ca variability in shallow water carbonates and the impact of submarine groundwater discharge on Ca-cycling in marine environments: Geochimica et Cosmochimica Acta, v. 83, p. 179–194, https://doi.org/10.1016 /j.gca.2011.12.031.
- Jones, D.S., Brothers, R.W., Ahm, A.-S.C., Slater, N., Higgins, J.A., and Fike, D.A., 2020, Sea level, carbonate mineralogy, and early diagenesis controlled δ<sup>13</sup>C records in Upper Ordovician carbonates: Geology, v. 48, p. 194–199, https://doi.org /10.1130/G46861.1.
- Kump, L.R., and Arthur, M.A., 1999, Interpreting carbon-isotope excursions: Carbonates and organic matter: Chemical Geology, v. 161, p. 181–198, https://doi.org/10.1016/S0009-2541(99)00086-8.
- Lau, K.V., Maher, K., Brown, S.T., Jost, A.B., Altıner, D., DePaolo, D.J., Eisenhauer, A., Kelley, B.M., Lehrmann, D.J., Paytan, A., Yu, M., Silva-Tamayo, J.C., and Payne, J.L., 2017, The influence of seawater carbonate chemistry, mineralogy, and diagenesis on calcium isotope variations in Lower–Middle Triassic carbonate rocks: Chemical Geology, v. 471, p. 13–37, https://doi .org/10.1016/j.chemgeo.2017.09.006.
- Maharjan, D., Jiang, G., Peng, Y., and Henry, R.A., 2018, Paired carbonate–organic carbon and nitrogen isotope variations in Lower Mississippian strata of the southern Great Basin, western United States: Palaeogeography, Palaeoclimatology, Palaeoecology, v. 490, p. 462–472, https://doi.org /10.1016/j.palaeo.2017.11.026.
- Mii, H., Grossman, E.L., and Yancey, T.E., 1999, Carboniferous isotope stratigraphies of North

- America: Implications for Carboniferous paleoceanography and Mississippian glaciation: Geological Society of America Bulletin, v. 111, p. 960–973, https://doi.org/10.1130/0016-7606(1999)111<0960:CISONA>2.3.CO;2.
- Myrow, P.M., Hasson, M., Taylor, J.F., Tarhan, L., Fike, D.A., Ramirez, G., Fowlkes, G., Popov, L.E., Liu, H., and Chen, J., 2023, Revised Paleozoic depositional history of the central Rocky Mountains (Utah and Colorado): Sedimentary Geology, v. 449, https://doi.org/10.1016/j.sedgeo .2023.106373.
- Oehlert, A.M., Swart, P.K., Eberli, G.P., Evans, S., and Frank, T.D., 2019, Multi-proxy constraints on the significance of covariant δ<sup>13</sup>C values in carbonate and organic carbon during the Early Mississippian: Sedimentology, v. 66, p. 241–261, https://doi.org/10.1111/sed.12502.
- Quinton, P.C., Rygel, M.C., and Bombard, S., 2023, Did sea level change drive carbon isotopic trends in the Madison Shelf? Sequence stratigraphy and carbon isotopes in the Mississippian Lodgepole Formation of southwest Montana: Palaeogeography, Palaeoclimatology, Palaeoecology, v. 628, https://doi.org/10.1016/j.palaeo.2023.111759.
- Saltzman, M.R., 2003, Organic carbon burial and phosphogenesis in the Antler foreland basin: An out-ofphase relationship during the Lower Mississippian: Journal of Sedimentary Research, v. 73, p. 844–855, https://doi.org/10.1306/032403730844.
- Saltzman, M.R., Groessens, E., and Zhuravlev, A., 2004, Carbon cycle models based on extreme changes in δ<sup>13</sup>C: An example from the Lower Mississippian: Palaeogeography, Palaeoclimatology, Palaeoecology, v. 213, p. 359–377, https://doi.org/10.1016/S0031-0182(04)00389-X.
- Staudigel, P.T., Higgins, J.A., and Swart, P.K., 2021, An abrupt middle-Miocene increase in fluid flow into the leeward margin Great Bahama Bank, constraints from  $\delta^{44}$ Ca and  $\Delta_{47}$  values: Earth and Planetary Science Letters, v. 553, https://doi.org/10.1016/j.epsl.2020.116625.
- Swart, P.K., 2008, Global synchronous changes in the carbon isotopic composition of carbonate sediments unrelated to changes in the global carbon cycle: Proceedings of the National Academy of Sciences of the United States of America, v. 105, p. 13,741–13,745, https://doi.org/10.1073/pnas .0802841105.
- Tang, J., Dietzel, M., Böhm, F., Köhler, S.J., and Eisenhauer, A., 2008, Sr<sup>2+</sup>/Ca<sup>2+</sup> and <sup>44</sup>Ca/<sup>40</sup>Ca fractionation during inorganic calcite formation: II. Ca isotopes: Geochimica et Cosmochimica Acta, v. 72, p. 3733–3745, https://doi.org/10.1016/j.gca.2008.05.033.
- Wang, J., Jacobson, A.D., Sageman, B.B., and Hurtgen, M.T., 2023, Application of the δ<sup>44,40</sup>Ca-δ<sup>88/86</sup>Sr multi-proxy to Namibian Marinoan cap carbonates: Geochimica et Cosmochimica Acta, v. 353, p. 13–27, https://doi.org/10.1016/j.gca.2023.04.023.
- Wilkinson, B.H., Owen, R.M., and Carroll, A.R., 1985, Submarine hydrothermal weathering, global eustasy, and carbonate polymorphism in Phanerozoic marine oolites: Journal of Sedimentary Research, v. 55, p. 171–183, https://doi.org/10.1306 /212F8657-2B24-11D7-8648000102C1865D.
- Yao, L., Qie, W., Luo, G., Liu, J., Algeo, T.J., Bai, X., Yang, B., and Wang, X., 2015, The TICE event: Perturbation of carbon-nitrogen cycles during the mid-Tournaisian (early Carboniferous) greenhouse-icehouse transition: Chemical Geology, v. 401, p. 1–14, https://doi.org/10.1016 /j.chemgeo.2015.02.021.

Printed in the USA